Dielectric properties of sols of silver nanoparticles capped by alkyl carboxylate ligands

G. F. Novikov, M. V. Gapanovich, E. V. Rabenok, L. M. Bogdanova, and L. I. Kuzub*

Institute of Problems of Chemical Physics, Russian Academy of Sciences, 1 prosp. Akad. Semenova, 142432 Chernogolovka, Moscow Region, Russian Federation. Fax: +7 (496) 522 1842. E-mail: ngf@icp.ac.ru

Sols of silver nanoparticles in toluene were studied by broadband dielectric spectroscopy (10^{-3}—10^5 Hz). The frequency dependences of the specific alternating current (ac) conductivity and the complex electric modulus were used to estimate the temperature/frequency intervals of long- and short-range charge transfer occurs, respectively. A considerable increase (by more than 30 °C) in the Vogel temperature T_0 and the glass transition temperature T_g in sols compared with the pure solvent was found. It can be hypothesized that these cooperative effects reflect the initial stage of the superlattice formation. Although the dielectric characteristics of sols are generally controlled by the conductivity relaxation, the dielectric response was observed in the high-frequency range (1—10^3 Hz) at low temperatures (from −50 to +10 °C). This response results from the presence of nanoparticles in solution. It is supposed that the relaxation is caused by the motion of ion impurities on the Ag nanoparticle surface within the carboxylate ligands shell. The dielectric properties of films strongly depend on both the characteristics of nanoparticles and the conditions of the film preparation. Like in sols, the direct current (dc) conductivity and the dielectric response of Ag nanoparticles in films are due to ion impurities.

Key words: sols of silver nanoparticles, broadband dielectric spectroscopy, chemical sensors.

As noted previously,[1] an important problem of the modern nanoindustry is the manufacture of stable monodisperse nanoparticles (NP) able to spontaneously form ordered 2D and 3D structures, so-called superlattices, upon concentration.[2] From this standpoint, silver NP are of considerable interest as they combine valuable optical, catalytic, and other properties and are readily accessible.[3] The currently known methods for the synthesis of silver NP[4] mainly imply the use of multicomponent dilute systems at silver ion concentrations of 10^{-3}—10^{-4} mol L^{-1}, which hampers isolation of reasonable amounts of NP from the final sol. Therefore, particular attention is attracted by the synthesis of silver NP by reducing silver carboxylates based on fatty acids with tertiary alklylamines first described by Yamamoto *et al*.[5] Characteristic features of the synthesis of silver NP from various low-molecular-weight carboxylates in triethylamine and their effect on the characteristics of the obtained NP were studied.[1] We made an attempt to investigate the initial stages of the self-assembly of NP in a sol.

Experimental

The synthesis and characteristics of samples have been described in detail previously.[1] Silver carboxylate based on saturated tetradecanoic acid $CH_3(CH_2)_{12}COOH$ was prepared by the reaction of the sodium salt of the acid with $AgNO_3$ in water. The carboxylate was reduced with triethylamine, which acted simultaneously as the reducing agent and as the reaction medium, at T = 348 K under argon. The resulting silver NP had a rather narrow size distribution and an average radius of 1 nm and were coated with a stabilizing ~1.8 nm-thick carboxylate ligand shell. The highest NP concentration in the samples was 0.036 g cm^{-3} of the sol. Toluene was used as the solvent.

The dielectric measurements were carried out on a Novocontrol broadband dielectric spectrometer in the frequency range of $f = 10^{-3}$—10^5 Hz and temperature range of 183—323 K. The sample temperature during the measurements was monitored to within 0.05 °C. The measuring cell comprised two gold-plated copper electrodes. The 50—200 μm gap between the electrodes was established by quartz spacers. The electrode diameter was 10—20 mm. The voltage between the electrodes did not exceed 1 V.

Results and Discussion

Frequency dependences of ε′, ε″, tanδ, and σ_{ac}′. Figures 1—4 show the frequency dependences of the real ε′ and imaginary ε″ parts of the complex dielectric permittivity $\varepsilon^* = \varepsilon' - j\varepsilon''$, tanδ, and the real part σ′ of the complex specific electrical conductivity $\sigma^* = \sigma' + j\sigma''$ in pure toluene and in NP sol in toluene at several temperatures from 183 to 223 K (here $j = \sqrt{-1}$). It can be seen that in pure

Published in Russian in *Izvestiya Akademii Nauk. Seriya Khimicheskaya,* No. 3, pp. 410—416, March, 2011.

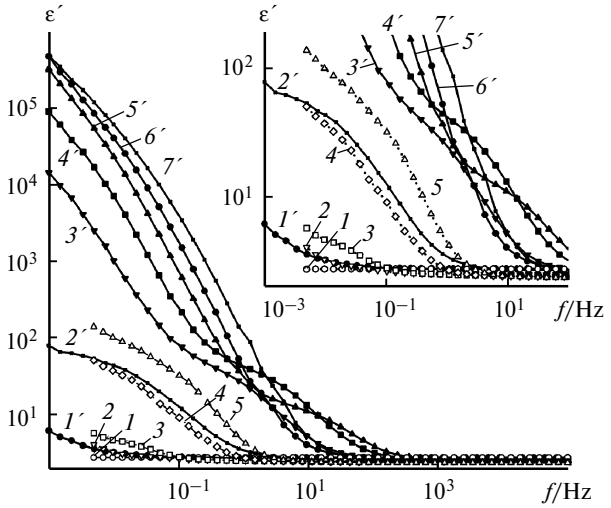

Fig. 1. Dependence of ε′ on frequency for pure toluene (*1*—*5*) and NP sol in toluene (*1′*—*7′*) at 183 (*1*, *1′*), 203 (*2′*), 223 (*3′*), 243 (*4′*), 263 (*2*, *5′*), 283 (*3*), 303 (*4*, *6′*), and 323 K (*5*, *7′*). The inset shows ε′(*f*) *vs.* frequency for 10^{-3}—10^2 Hz.

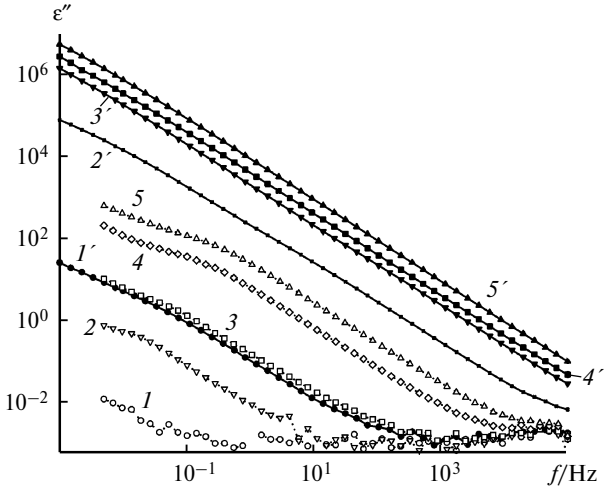

Fig. 3. Dependence of ε″ on frequency for pure toluene (*1*—*5*) and NP sol in toluene (*1′*—*5′*) at 183 (*1*, *1′*), 223 (*2*, *2′*), 263 (*3*, *3′*), 303 (*4*, *4′*), and 323 K (*5*, *5′*).

toluene at low frequencies and high temperatures, ε′, ε″, and tanδ increase by several orders of magnitude compared with these values characteristic of dipole relaxation and they should be attributed to the conductivity relaxation and spatial charge polarization.[6—8] The reason for these phenomena is charge migration between the electrode surface and the sample.

Apart from conductivity relaxation and spatial charge polarization, high ε′, ε″, and tanδ values in the low frequency range may be caused by Maxwell—Wagner—Sillars—Weiss (MWSW) polarization and relaxation, which are observed in microphase-separated systems. The MWSW polarization is caused by polarization in the sample bulk at the interface of two phases with different conductivities and permittivities. Due to high conductivity of Ag particles, the characteristic frequency of relaxation of MWSW polarization (MWSW relaxation) of a single silver NP occurs at GHz frequencies (*i.e.*, beyond our frequency range).[9] However, it is possible that from the microphase separation standpoint, it is necessary to consider coated silver NP rather than NP as such. These complex particles are much larger, and their dielectric characteristics can differ considerably from characteristics of metallic NP. As a result, it may happen that the corresponding MWSW polarization/relaxation effects would be manifested in an available temperature/frequency range.

In the case of MWSW relaxation/polarization, the corresponding frequency dependences of ε″ usually have

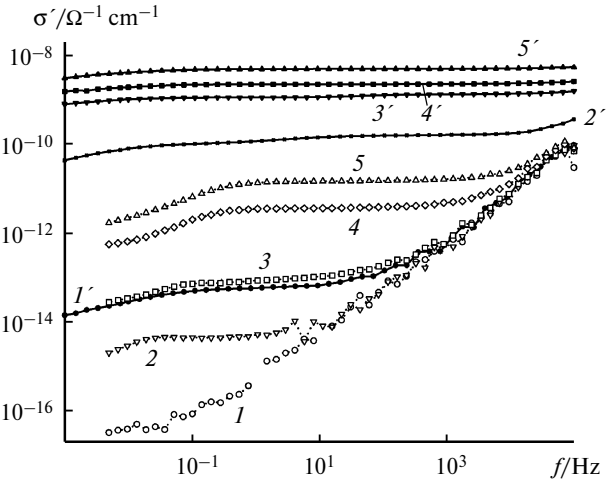

Fig. 2. Dependence of σ′ on frequency for pure toluene (*1*—*5*) and NP sol in toluene (*1′*—*5′*) at 183 (*1*, *1′*), 223 (*2*, *2′*), 263 (*3*, *3′*), 303 (*4*, *4′*), and 323 K (*5*, *5′*).

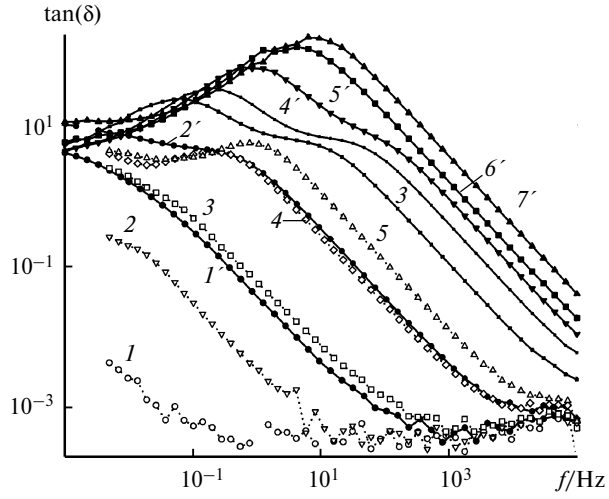

Fig. 4. Dependence of tan(δ) on frequency for pure toluene (*1*—*5*) and NP sol in toluene (*1′*—*7′*) at 183 (*1*, *1′*), 203 (*2′*), 223 (*2*, *3′*), 243 (*4′*), 263 (*3*, *5′*), 303 (*4*, *6′*), and 323 K (*5*, *7′*).

a maximum in the region where a step is recorded for ε′ ($\Delta\varepsilon \approx 10$—$20$ irrespective of temperature). As the temperature increases, the peak and the step shift to higher temperature.[10] As can be seen from Fig. 1, for NP sol, the right wings of the curves have steps that shift to higher temperature. However, it is impossible to draw conclusion about the step amplitude variation *vs.* temperature on the basis of these data due to the overlap of conductivity relaxation and spatial charge polarization processes, which becomes more pronounced as the temperature is increased.

For further elucidation of the issue whether the MWSW polarization/relaxation is responsible for increase in ε′, ε″, and tanδ in the low-frequency/high-temperature region, consider the frequency dependence of the specific conductivity σ'_{ac}. As for other concentrations, the plot $\log\sigma'_{ac} = \varphi(\log f)$ (see Fig. 2) has a clear-cut plateau at low frequency, which extends to higher frequency as the temperature increases; this is attributable to free charge transport.[11]

The conductivity values σ'_{ac} in the plateau region correspond to the direct current (dc) conductivity σ_{dc} both in pure toluene and in the sol. The transition from the plateau region to the frequency dependence of σ'_{ac} (at the frequency f^*) corresponds to a change in the mechanism of electrical conductivity.[11,12] In this case, the plateau region in the left-hand part of the plot $\log\sigma'_{ac} = \varphi(\log f)$ reflects the charge transport by long distances, while in the right-hand part, the σ'_{ac} values increase with increase in the frequency and the charge transport is restricted to the space of their potential wells.

The frequency region of σ_{dc} (see Fig. 2) corresponds to the region of high ε″ values (see Fig 3). In the low frequency/high temperature region, all of the studied systems show the linear dependence $\log\varepsilon'' = \varphi(\log f)$ with a slope close to −1. This behavior is typical of the conductivity relaxation.[9,11] Therefore, one can expect that a sharp increase in the dielectric loss (see Fig. 3) is related to the dc conductivity, and MWSW polarization does not make a noticeable contribution to this increase.

Thus, in the low-frequency/high-temperature region, the frequency dependences of σ_{ac}' (see Fig. 2), ε″ (see Fig. 3), and tanδ (see Fig. 4), show the following features: deviation from the linearity of ε″, a maximum of tanδ, and a slight decrease in σ_{ac}'. The described features of dielectric behavior are typical of electrode polarization associated with charge accumulation at the interface between the sample and the electrodes.[11,13—16] Note, however, that the tanδ(*f*) plots (see Fig. 4) of NP sols exhibit also the second maximum at the high-frequency wing whose behavior correlates with the step in the frequency dependences of ε″ (see Fig. 3). In a pure solvent, no maximum is observed. On temperature rise, the maximum shifts to high-frequency region. The amplitude of this maximum depends little on the temperature.

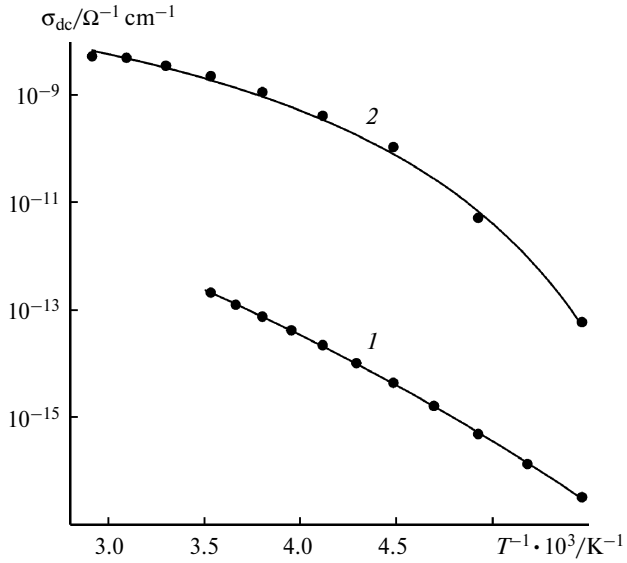

Fig. 5. Vogel—Fulcher—Tammann dependence for pure toluene (*1*) and NP sol in toluene (0.036 g cm^{-3}) (*2*).

Temperature dependence of the specific conductivity. It is known that in many glass-forming media, the experimental dependences of the specific conductivity and dielectric relaxation times on the reciprocal temperature are not described by the Arrhenius law. Most often, the empirical Vogel—Fulcher—Tammann (VFT) formula is used in this case:[6]

$$\sigma_{dc} = \sigma_{dc0}\exp[-B/(T - T_0)], \quad (1)$$

where σ_{dc0}, B , and T_0 are the adjustable parameters, T_0 is the so-called Vogel—Fulcher temperature often interpreted as the "static freezing" temperature of electric dipoles or the transition temperature to the dipole glass state[17,18] (T_0 is usually lower than the glass transition temperature T_g by several tens of degrees[19]).

The plots $\log\sigma_{dc} = \varphi(1/T)$ for pure toluene and for the NP sol in toluene (0.036 g cm^{-3}) are shown in Fig. 5. They are described quite satisfactorily by the VFT function (solid lines). This fact implies that on decreasing the temperature, the change in the system viscosity is considerably affected by cooperative motion.

The temperature dependence of the dc conductivity is described by the relation[20]

$$\sigma_{dc} = \sigma_{dc0}\exp[-DT_0/(T - T_0)], \quad (2)$$

where D is the so-called strength parameter, the D value can be used to estimate the system fragility.

The fragility concept was introduced to take into account the thermodynamic and kinetic aspects of glass transition. The parameter D characterizes the deviation of the temperature dependence $\log\sigma_{dc} = \varphi(1/T)$ from the Arrhenius linear dependence. The greater the deviations of the plot $\log\sigma_{dc} = \varphi(1/T)$ from the straight line,[8] the lower the

D values. For example, for "stable systems" including ionic glasses, the plot $\log\sigma_{dc} = \varphi(1/T)$ is nearly linear and *D* reaches 100. For covalent glasses and polymers, this dependence is non-linear and *D* values are 30 and 5—20, respectively.[20,21]

The parameters $\log\sigma_{dc0}$, *D*, and T_0 for the NP sol in toluene system are summarized in Table 1. It can be seen that with increase in the NP concentration, the parameter *D* decreases. This fact indicates that as the NP concentration increases, their influence on the sol properties increases and the charge transport in the NP-containing sol is correlated with the molecular motion of sol particles and its behavior reflects the increase in the role of cooperative effects.

Having determined *D*, it is possible to estimate the glass transition temperature T_g with the assumption that for both pure toluene and sols, the following relation holds:[22]

$$T_g = T_0(1 + 0.0255D).$$

It can be seen from Table 1 that upon the addition of silver NP in a concentration of 0.036 g cm^{-3}, the glass transition temperature increases by 33 K.

It is of interest to find out how the T_g values that we determined by dielectric spectroscopy are related to the values determined by other methods and published previously. It was found that the T_g values we determined (see Table 1) are 7—10 K higher than the published data: for pure toluene, $T_g = 114$ (see Ref 23) and 117 K (see Ref. 24). It is unknown as yet what is the reason for the observed difference and whether relation holds for our system. One might suggest that in a measuring cell with metallic electrodes and Teflon spacers, it is difficult to ensure the absence of ionic impurities at high level. However, control experiments did not support this suggestion. Probably, the differences in T_g for toluene are due to the specific conditions of sample freezing/thawing.

Unfortunately, there are no published data on T_g for silver NP sols in toluene. However, the detected increase in T_g in the sol as compared with pure toluene indicates that the glass transition in the sol differs considerably from the glass transition in pure toluene.

Effect of silver NP on the specific conductivity and dielectric permittivity of the sol. As noted above, upon the addition of NP in toluene, the plots of ε′ *vs.* frequency show a feebly pronounced inflection at $f < 10^2$ Hz (see Fig. 1), the position of the inflection point shifting to lower frequency as the temperature is decreased. This inflection point is correlated with the position of the high-frequency maximum in the frequency dependences of tanδ (see Fig. 4). In addition, as the NP concentration increases, the plateau in the frequency dependences of σ_{ac} extends to higher frequencies and the σ_{dc} value increases (the frequency of transition from dc to ac conductivity (*f**) increases by more than an order of magnitude).

It can be seen from Fig. 2, at a nanoparticle concentration of 0.036 g cm^{-3}, the σ_{dc} value at 223 K increases by more than two orders of magnitude. However, σ_{dc} still remains low (~10^{-9} Ω^{-1} cm^{-1}) and rather typical of dielectrics and not of percolating systems. The volume fraction of silver NP coated by shells made of acid residues for the concentration of 0.036 g cm^{-3} (see Table 1) is estimated as ~4%, which is considerably lower than the theoretical percolation threshold of 16 vol.% (at a random distribution of spherical particles in the three-dimensional system[25]). Even a lower volume fraction is obtained if uncoated particles are considered. This provides the conclusion that the jumps of electrons from one silver NP to another are unlikely in this system. Thus, at these NP concentrations, no percolation bridges are apparently formed. Otherwise, the conductivity would have increased by several orders of magnitude.

Thus, analysis of the plot $\log\sigma'_{ac} = \varphi(\log f)$ (see Fig. 2) made it possible to estimate σ_{dc} under various experimental conditions and to determine the limits of operation of the conductivity mechanism where charge carriers can travel by short and long distances. As noted above, the conductivity is provided by ions that move in the solvent (and partially in the NP shell made of acid residues) to a higher extent than by the electrons of silver particles. An additional reason supporting this issue is the temperature dependence of the dc conductivity (see Fig. 5), which attests to the crucial influence of the molecular motion of the solvent on the conductivity mechanism.

Table 1. VFT parameters from relation (2) for toluene and a silver nanoparticle sol (0.036 g cm^{-3})

Sample	Calculation method	$-\log\sigma_{dc0}$	$\log(\tau_{max,M''}^{-1})$	T_0/K	*B*	*D*	T_g/K
Toluene	*A**	8.40	—	71	2098	29.5	124
Silver NP in toluene (0.036 g cm^{-3})	*A**	6.86	—	142	602	4.2	157
	*B***	—	5.9	143	617	4.3	159

* From the data of Fig. 5 and T_g parameters found from relation (3).

* In view of data on $\tau_{max,M''}$ (see Fig. 7), the results of calculations using relation (9), and the data of Fig. 8.

Thus, it can be concluded that the NP concentration in our sols is below the percolation threshold and the particle distribution should be considered rather uniform. In this case, according to the percolation theory, the conductivity away from the threshold should differ little from the solvent conductivity. However, in experiments, a real increase in the conductivity with increase in the NP concentration is observed. Meanwhile, the data of Fig. 5 provide grounds to believe that the conductivity is performed by the ions whose motion is controlled by the molecular motion in the sol. The conductivity value is determined by the mobilities and concentrations of ions. Therefore, high dc conductivity values in the studied sols are apparently caused by the impurities arising during the sample preparation. However, the observed step in the high-frequency part of the ε′ curves (see Fig. 1) and the high-frequency maximum of the tanδ curves (see Fig. 4), which are missing in toluene but are manifested in NP sols, are attributable to dielectric relaxation caused by nanoparticles.

Complex electric modulus. The measured ε′ and ε″ values can be converted to the complex electric modulus (M^*) expressed by the equation

$$M^*(i\omega,T) = [\varepsilon^*(i\omega,T)]^{-1} = M'(i\omega,T) + iM''(i\omega,T), \qquad (4)$$

where

$$M' = \varepsilon'/(\varepsilon'^2 + \varepsilon''^2) \qquad (5)$$

and

$$M'' = \varepsilon''/(\varepsilon'^2 + \varepsilon''^2). \qquad (6)$$

Here M' and M'' are the real and imaginary components of the complex electric modulus. The frequency dependences of the imaginary part of M^* for pure toluene and NP sol are shown in Fig. 6. It can be seen that the introduction of NP in toluene results in the shift of maxima to higher frequencies. An increase in the frequency of the maxima is clearly observed upon increase in temperature, which attests to their relaxation character.

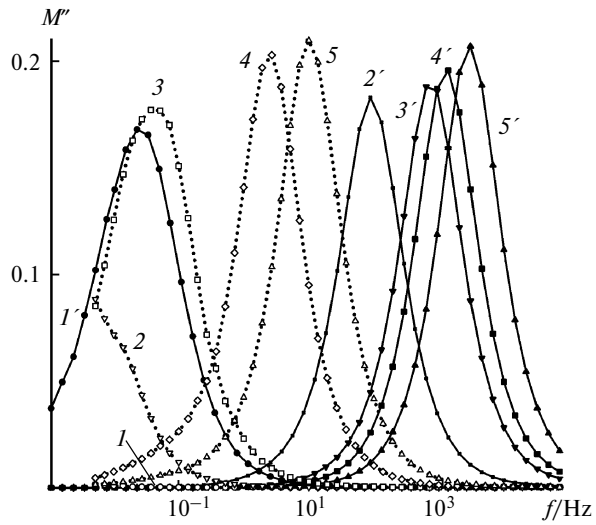

Fig. 6. Frequency dependence of M″ for pure toluene (*1*—*5*) and NP sol in toluene (*1′*—*5′*) at 183 (*1*, *1′*), 223 (*2*, *2′*), 263 (*3*, *3′*), 303 (*4*, *4′*), and 323 K (*5*, *5′*).

In order to understand the molecular mechanism of the discussed process, compare the frequency dependences of M'' and σ_{ac}. At identical temperatures, the frequency of the maximum of M'' is close to that for f^* in all of the studied systems. This trend has also been observed previously in other systems and was attributed to the relaxation conductivity.[11,26] Apparently, this situation also occurs in this case. With this assumption, the frequencies of the M'' maxima (see Fig. 6) should separate the regions of short- and long-order charge mobility, which are located on the right and on the left of the maximum, respectively.

When the M^* value is completely caused by ionic conductivity, it is related to the Maxwell relaxation time or the conductivity relaxation time τ_σ as follows:

$$M^*(i\omega,T) = M_0 i\omega\tau_\sigma(T)/[1 + i\omega\tau_\sigma(T)], \qquad (7)$$

where $\tau_\sigma = e_0\varepsilon_0/\sigma_{dc}$, σ_{dc} is the dc conductivity and $M_0 = \varepsilon_0^{-1}$. In Eq. (7), the M^* value is invariant with respect to ω and τ_σ (or equivalent to σ_0), and M' and M'' obey the equation

$$[M''(\omega,T)]^2 + [M'(\omega,T) - M_0(T)/2]^2 = [M_0(T)/2]^2. \qquad (8)$$

The plot of M'' *vs.* M' is a semicircle with the radius of $0.5M_0$ and the center in the M' axis if ω and T are chosen in such a way that no processes other than ionic conductivity make a contribution to $\varepsilon^*(i\omega,T)$. Otherwise, the shape of the plot deviates from the semicircle.

Thus, the observed semicircle in the M^* data representation attests to the Debye relaxation with the only relaxation time τ, so that at the semicircle maximum

$$\omega\tau_{\max,M''} = 1; \qquad (9)$$

here the alternating current electric field conductivity is equal to the direct current field conductivity. This situation was found to arise in both pure toluene and NP sol (Fig. 7). It can be seen that the data fit satisfactorily to the semicircle centered on the *x*-axis.

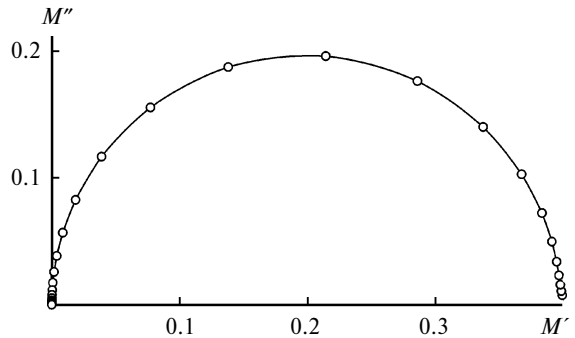

Fig. 7. Diagram $M''(M')$ for NP sol in toluene at $T = 283$ K.

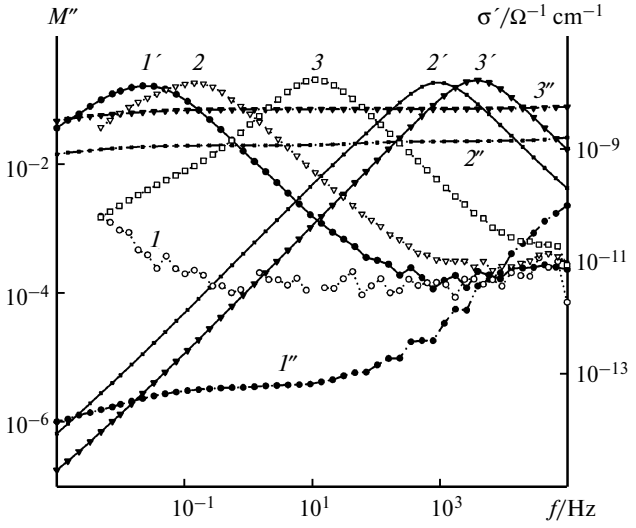

Fig. 8. Dependence of M'' on frequency for pure toluene (*1—3*) and M'' (*1′—3′*) and σ' (*1″—3″*) on frequency for NP sols in toluene.

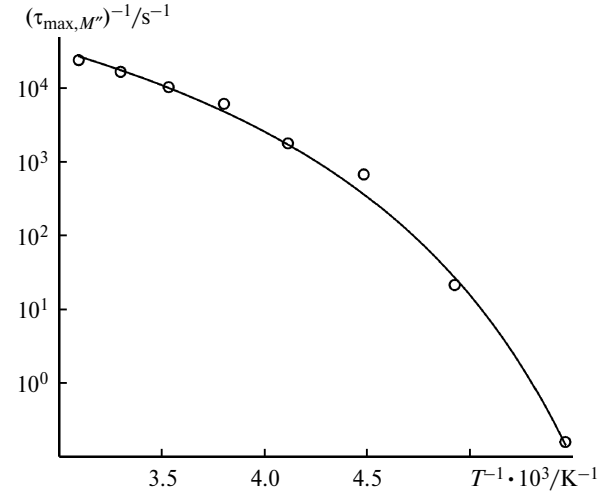

Fig. 9. Dependence of $\tau_{max,M''}^{-1}$ on the reciprocal temperature for NP sol in toluene (0.036 g cm^{-3}).

The plots $\log(M'') = \varphi(\log f)$ are presented in Fig. 8. It can be seen that in these coordinates, the M'' values on the left of the maximum depend linearly on the frequency, while in the right-hand part a feebly pronounced maximum is observed at high frequencies $f > 10^5$ Hz. The onset of the transition is consistent with the transition frequency from the dc to ac conductivity $f^* \approx 10^2$ Hz. In view of this result, the low-frequency peak can be assigned to the conductivity relaxation and the less pronounced high-frequency peak can be assigned to the relaxation of dipole polarization.

The conductivity relaxation times found from the data of Fig. 7 are shown in Fig. 9 as the functions of the reciprocal temperature. The results of adjustment of the temperature dependence of $\tau_{max,M''}$ are presented in Fig. 9 and in Table 1 (calculation from Eq. (3)). The results are in satisfactory agreement with the data of Fig. 5 and Table 1 (calculation from Eq. (2)); this is not surprising, as both reflect the free charge conductivity relaxation process.

The dielectric response of nanoparticles. As noted above, some facts are indicative of the dipole relaxation in the NP sols, which is not always clearly seen due to high dc conductivity. In particular, this is a step in the high-frequency region of the ε' curves (see Fig. 1) and the high-frequency maximum in the tanδ plots (see Fig. 4), which are not recorded in toluene but are manifested in the NP sols. The presence of dipole relaxation is also indicated by the feebly pronounced maxima in the range of $1—10^3$ Hz in the frequency dependences of the conductivity (see Fig. 2). These features are not observed in the pure solvent and, hence, they are undoubtedly attributable to the NP.

It is natural to believe that the positions of maxima in the frequency dependences of ε' (see Fig. 1) and tanδ (see Fig. 4) are described, at least roughly, by the condition $2\pi f_{NP}\tau_{NP} = 1$, where $f_{NP} = 1—10^3$ Hz, τ_{NP} is the relaxation time. As noted above, τ_{NP} cannot be related to the electronic conductivity of the silver NP, because this time is five to six orders of magnitude longer than that expected in the case of electronic conductivity. However, since the NP are coated, the dipole polarization/relaxation may be provided by ions that move in the shell. Let us estimate the necessary mobility of ions in this model. For a 200 μm thick sample, the electric field strength $E = 50$ V cm^{-1} (without allowance for the depolarization factor). Assuming the radius of the silver NP and the shell thickness to be 1 and 1.8 nm (13 bond lengths 0.14 nm each), the drift length along the shell can be estimated as ~1—6 nm. For observance of the time-of-flight conditions for ion mobility in the range $T = 223—283$ K, one gets

$$\mu_i = l(\tau_{NP}E)^{-1} = 2\pi f_{NP} l/E \approx 10^{-7}—10^{-4}\ \text{cm}^2\ \text{V}^{-1}\ \text{s}^{-1}.$$

The obtained estimate does not contradict the typical values of ion mobility in liquid media and can justify the proposed model.

Thus, we presented the results of dielectric studies of silver NP sols in toluene at low frequency ($10^{-3}—10^5$ Hz). Using the frequency dependences of the ac conductivity σ'_{ac} and the imaginary part of the complex dielectric modulus M'', the boundaries of the temperature/frequency ranges where long- and short-range charge transfer takes place were estimated. On increase in the silver NP concentration, the direct current conductivity σ_{dc} increases; however, even at the highest NP concentrations in the sol (0.036 g cm^{-3}), the percolation threshold is not reached and no electron conductivity is found either. The σ_{dc} curves *vs.* temperature showed pronounced deviation from the Arrhenius plot, which attests to a considerable contribution of cooperative effects to the charge transport mechanism. A considerable (33 K) increase in the Vogel—Fulcher—Tam-

mann temperature (T_0) and glass transition temperature T_g in the sols compared with the pure solvent was found. Apparently, the cooperative effects reflect the initial stage of formation of superlattices. Although the dielectric characteristics of the sols were mainly controlled by the conductivity relaxation, a dielectric response caused by the presence of NP in the sol was observed at $1—10^3$ Hz between −50 and +10 °C. Analysis of the data suggests that the ion motion over the silver NP surface within the carboxylate ligand shell is responsible for the relaxation.

The authors are grateful to P. V. Buzin for the aid in performing the experiments and to V. I. Irzhak for useful discussion and valuable advice concerning the work.

This work was supported by the Russian Foundation for Basic Research (Project No. 08-03-12088_ofi).

References

1. L. I. Kuzub, L. M. Bogdanova, T. S. Kurkin, V. I. Torbov, L. I. Gur´eva, B. A. Rozenberg, P. V. Buzin, in *Struktura i dinamika molekulyarnykh sistem* (*Structure and Dynamics of Molecular Systems*), Mari State Technical University, Ioshkar-Ola—Ufa—Kazan´—Moscow, 2009, XVI, ch. 2, p. 134.
2. B. A. Rozenberg, R. Tenne, *Progr. Polym. Sci.*, 2008, **33**, 40.
3. A. Henglein, *Chem. Rev.*, 1989, **89**, 1861.
4. Yu. A. Krutyakov, A. A. Kudrinskii, A. Yu. Olenin, G. V. Lisichkin, *Usp. Khim.*, 2008, 242 [*Russ. Chem. Rev.* (*Engl. Transl.*), 2008, **77**, 233].
5. M. Yamamoto, Y. Kashiwagi, M. Nakamoto, *Langmuir*, 2006, **22**, 8581.
6. F. Kremer, in *Broadband Dielectric Spectroscopy*, Ed. A. Schonhals, Springer-Verlag, Berlin, 2003, Ch. 3.
7. I. A. Chernov, T. R. Deberdeev, G. F. Novikov, R. M. Garipov, V. I. Irzhak, *Plasticheskie massy*, 2003, No. 8, 5 [*Inter. Polym. Sci. Tech.* (*Engl. Transl.*), 2004, **31**, No. 5, 17].
8. N. A. Nikonorova, E. B. Barmatov, D. A. Pebalk, M. A. Barmatova, G. Dommguez-Espinosa, R. Diaz-Calleja, P. Pissis, *J. Phys. Chem. C*, 2007, **111**, 8451.
9. P. Hedvig, *Dielectric Spectroscopy in Polymers*, Adam Hilger, Bristol, England, 1977.
10. C. Tsonos, L. Apekis, K. Viras, L. Stepanenko, L. Karabanova, L. Sergeeva, *Solid State Ion.*, 2001, **143**, 229.
11. P. Pissis, A. Kyritsis, *Solid State Ion.*, 1997, **97**, 105.
12. K. Yamamoto, H. Hamikawa, *Jpn J. Appl. Phys.*, *Part 1*, 1988, **27**, 1845.
13. G. A. Shandryuk, A. V. Rebrov, R. B. Vasiliev, S. G. Dorofeev, A. S. Merekalov, A. M. Gas´kov, R. V. Talroze, *Polym. Sci. B*, 2005, **47**, 266.
14. I. D. Raistric, in *Impedance Spectroscopy*, Ed. J. R. Macdonald, Wiley, New York, 1987, Ch. 2.
15. K. Miyairi, *J. Phys. D*, 1986, **19**, 1973.
16. E. Neagu, P. Pissis, L. Apekis, *J. Appl. Phys.*, 2000, **87**, 2914.
17. K. N. Fisher, *Phys. Status Solidi. B*, 1983, **116**, 357.
18. D. Viehland, S. Jang, L. E. Cross, M. Wuttig, *Phil. Mag. B.*, 1991, **64**, 335.
19. R. Richert, C. A. Angell, *J. Chem. Phys.*, 1998, **108**, 9016.
20. C. A. Angell, *J. Non-Cryst. Solids*, 1991, **13**, 131.
21. R. Boehmer, K. L. Ngai, C. A. Angell, D. J. Plazek, *J. Chem. Phys.*, 1993, **99**, 4201.
22. C. A. Angell, *Annu. Rev. Phys. Chem.*, 1992, **43**, 693.
23. A. Kh. Vorob´ev, V. S. Gurman, Yu. B. Kheifets, *Vestn. Mosk. Univ.*, *Ser. 2. Khim.*, 2008, **49**, 7 [*Vestn. Mosk. Univ.*, *Ser. Khim.* (*Engl. Transl.*), 2008, **49**].
24. M. Murai, H. Nakayama, K. Ishii, *J. Therm. Anal. Calor.*, 2002, **69**, 953.
25. D. Stauffer, A. Aharony, *Introduction to Percolation Theory*, Taylor and Francis, London, 1992.
26. E. Neagu, P. Pissis, L. Apekis, J. L. Gomes Ribelles, *J. Phys. D: Appl. Phys.*, 1997, **30**, 1551.

Received August 9, 2010;
in revised form February 2, 2011